UNIVERSIDAD NACIONAL AUTÓNOMA DE MÉXICO

FACULTAD DE QUÍMICA

ANÁLISIS DE LA POLIMERIZACIÓN RADICÁLICA POR TRANFERENCIA DE ATOMO ACTIVADA POR MICROONDAS DE METACRILATO DE METILO Y ESTIRENO USANDO HERRAMIENTAS DE MODELACIÓN
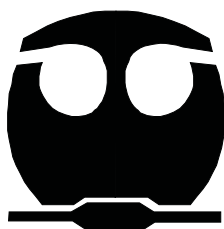
ACTIVIDAD DE INVESTIGACIÓN

QUE PARA OBTENER EL TÍTULO DE:

INGENIERIO QUÍMICO

P R E S E N T A:

PORFIRIO LÓPEZ DOMÍNGUEZ

MÉXICO D. F.   2013

JURADO ASIGNADO:

PRESIDENTE:	Dr. Joaquín Palacios Alquisira
VOCAL:	M. en C. Marco Antonio Uresti Maldonado
SECRETARIO:	Dr. Eduardo Vivaldo Lima
1er. SUPLENTE:	Dr. Francisco López Serrano Ramos
2° SUPLENTE:	Dr. Martín Rivera Toledo

SITIO DONDE SE DESARROLLÓ EL TEMA:

Laboratorio de Reactores de Polimerización D-324B

Departamento de ingeniería química, Facultad de Química, Universidad Nacional Autónoma de México

ASESOR DEL TEMA:

Dr. Eduardo Vivaldo Lima

_____

SUSTENTANTE:

Porfirio López Domínguez

_____

CONTENIDO

Protocolo de Investigación

Tema

Análisis de la polimerización radicálica por transferencia de átomo activada por microondas de metracrilato de metilo y estireno usando herramientas de modelación

Introducción

Con el fin de obtener productos poliméricos más homogéneos se han desarrollado técnicas de síntesis controladas (CP). Las más importantes son ATRP (Polimerización radicálica por transferencia de átomo), NMR (Polimerización radicálica mediada por nitróxidos) y RAFT (Polimerización por transferencia adición-fragmentación reversible). En el caso de ATRP se usa un sistema de iniciación que consta de un iniciador y un catalizador, que comúnmente es un haluro de alquilo y un ligante. Este iniciador experimenta una reacción reversible que proporciona control al sistema de polimerización. Una desventaja de las polimerizaciones controladas es el hecho de que la rapidez de polimerización es baja en comparación con las correspondientes síntesis convencionales (iniciador y monómero). Una manera de revertir esta desventaja es usar un reactor de microondas para acelerar la reacción. Los primeros reactores de microondas fueron modificaciones de hornos de microondas comerciales que usaban sensores de infrarrojo para medir la temperatura del sistema. Se ha demostrado en algunos trabajos que a veces las temperaturas leídas eran subestimadas, sugiriendo que la verdadera temperatura de reacción es más alta y que los "efectos microondas" se debían a ello. Actualmente, los reactores pueden ser equipados con sensores de fibra óptica, los cuales permiten una lectura de la temperatura más cercana a la real. Se ha visto que en sistemas con buen control de temperatura la rapidez de reacción no aumenta en

1

comparación con las polimerizaciones con calentamiento convencional. Esta situación ha llevado a un debate sobre el verdadero efecto del calentamiento en microondas, es decir, si las mejoras se deben a una modificación en el esquema de polimerización o si el efecto es puramente térmico. En polimerizaciones por NMR o RAFT se han reportado cambios bruscos en la rapidez de polimerización; los investigadores atribuyen este fenómeno al "efecto microondas" y afirman que la polimerización ocurre a temperatura constante. En contraste, otras polimerizaciones activadas por microondas han mostrado ausencia del "efecto microondas". Es debido a esta discusión que se propusieron dos modelos. El primero de ellos, el cual denominaremos Modelo 1, toma en cuenta la generación de radicales a partir del monómero, es decir, un monómero produce dos radicales, y el segundo, denominado Modelo 2, toma en cuenta variaciones de temperatura en el sistema. También se realizaron algunas simulaciones combinando ambos modelos. Para facilitar los cálculos numéricos se usó el paquete de simulación Predici, de CiT. Con esta herramienta se pueden realizar análisis de sensibilidad para evaluar el comportamiento de los sistemas bajo irradiación por microondas y contrastar con resultados experimentales.

Objetivos de la investigación

1. Implementar la polimerización ATRP en el paquete de simulación Predici.

2. Estudiar las polimerizaciones ATRP de Metacrilato de Metilo y Estireno bajo calentamiento convencional.

3. Analizar las polimerizaciones ATRP de Metacrilato de Metilo y Estireno bajo irradiación por microondas.

4. Contrastar los resultados numéricos con datos experimentales obtenidos de la literatura.

Materiales y Métodos

El esquema de reacción de la polimerización ATRP comprende un conjunto de reacciones elementales de las cuales se destaca la participación de un sistema iniciador/catalizador. El uso de este iniciador permite reducir la cantidad de radicales libres en el sistema favoreciendo la propagación de radicales en vez de la terminación por combinación y desproporcionación de radicales poliméricos. El esquema completo se implementó en el simulador de procesos macromoleculares Predici, de CiT. En Predici cada reacción es presentada como "un paso". Cada reacción elemental está asociada con una constante cinética. Estas constantes cinéticas fueron buscadas en la literatura, principalmente de experimentos con pulsos de láser. Los monómeros de interés son metacrilato de metilo y estireno por sus aplicaciones industriales y por el gran cúmulo de información sobre ellos. Se buscaron sistemas donde se conocieran la dependencia de los parámetros con la temperatura. Dado que algunas polimerizaciones ATRP fueron realizadas en masa, fue necesario tomar en cuenta el efecto Trommsdorf o efecto de autoaceleración. Se usó la teoría de volumen libre para abordar este fenómeno. Se obtuvieron los parámetros "beta" para las reacciones de propagación y terminación por combinación/ desproporcionación a partir de polimerizaciones en masa. Los parámetros estimados en la polimerización ATRP fueron los parámetros de volumen libre ("betas") para las reacciones de activación y desactivación así como la constante de desactivación bajo calentamiento convencional. Para el Modelo 1 se estimó la constante cinética de irradiación, en el caso del Modelo 2 se estimaron las temperaturas finales.

Analysis of the Microwave Activated Atom Transfer Radical Polymerization of Methyl Methacrylate and Styrene using Modeling Tools[¥]

Porfirio López-Domínguez and Eduardo Vivaldo-Lima*

_____

P. López-Domínguez, Prof. Dr. E. Vivaldo-Lima
Facultad de Química, Departamento de Ingeniería Química, Universidad Nacional Autónoma de México, 04510 México D.F., México, Fax: +5255-5622-5355, E-mail: vivaldo@unam.mx

_____

Abstract. The effect of microwave irradiation (MI) on the kinetics and molecular weight development in the atom transfer radical polymerization (ATRP) of methyl methacrylate (MMA) and styrene is studied by using modeling tools. Two models are proposed; one captures the "microwave effect" through a microwave-activated radical generation from monomer reaction, besides the typical reactions involved in the polymerization scheme for ATRP, and the other considers non-constant predefined temperature profiles for the polymerization scheme of ATRP ("thermal effect" model). It is found that both models can reproduce equally well the experimental behavior and performance of several systems reported in the literature. So, more experimental and modeling studies are needed to actually discriminate between the two models.

* Author whom correspondence should be addressed

Introduction

The area of controlled radical polymerization (CRP) (or reversible-deactivation radical polymerization (RDRP), which is the IUPAC recommended term[1])is nowadays well established and mature. Polymerization techniques such as ATRP,[2] nitroxide-mediated radical polymerization (NMRP)[3] and reversible addition-fragmentation chain transfer (RAFT)[4] polymerization are useful in the synthesis of macromolecules with designed and controlled microstructures and complex architectures, including hybrids with inorganic components and bioconjugates for diverse applications.[2] One disadvantage with most RDRP systems is the fact of having low polymerization rates, compared to the corresponding conventional free radical (RP) counterparts. One way to try to overcome such disadvantage is the use of microwave irradiation to speed up the polymerization rate. There are several reports in the literature on MI-activated RDRP polymerizations by ATRP,[5-16] RAFT[17-22] and NMRP.[23-25] In these reports it is usually observed that polymerization rate is moderately to dramatically improved, depending on the level of temperature control attained in the microwave synthesis equipment. Moderate increases in polymerization rate are usually observed in cases where the polymerizationsare carried out in microwave synthesis devices specificallydesigned for organic syntheses and with carefully controlled temperature profiles,[12,23,24,26,27] whereas the more spectacular increases in polymerization rate have been usually observed in domestic or self-modified domestic microwave ovens.[6,8-11,13-16,22] This situation has led to a debate in the literature on the true effect of MI on RP and RDRP, namely, if there is a true

"microwave effect" (a modification on the polymerization scheme or a specific reaction with an unusually high kinetic rate constant, both attributable to MI),[16,28,29] or if the actual effect of MI on these polymerizations is purely thermal (non-constant temperature profiles caused by MI).[12,23,24,26,27,30]

Kwak et al.[26] carried out a critical comparison of RP under conventional heating (CH) and microwave heating (MWH) and observed, for the case of RP of methyl methacrylate (MMA) under MWH, that the polymerization was only slightly faster under precise temperature control using a dually temperature-controlled reaction vessel (DTRV), and the resulting polymer had only smaller number average molecular weight (M_n) values. They also observed that the decomposition rates of 2,2'-Azobis(isobutyronitrile) (AIBN) under CH and MWH with precise temperature control were essentially identical, and for the cases of random copolymerizations of MMA with styrene (St), butyl acrylate (BA) and 4-acetoxystyrene (AcSt), the copolymer compositions were exactly the same. They concluded that rate enhancement is mostly due to higher temperature of the reaction mixture than the temperature observed on the instrument display.

In our group, we have theoretically studied the performance of RDRP systems carried out under MWH with the aid of modeling tools. We presented the first modeling studies for emulsion RP,[31,32] NMRP[33] and RAFT[34] polymerizations activated with MI (or under MWH if there is no actual activation). More recently, the case of RAFT polymerization under MWH has also been modeled by Zetterlund and Perrier.[35] In our modeling studies, the "microwave effect" has been captured by considering a reaction of microwave-activated radical generation from

6

monomer,[31,33,34] or radical generation from a hypothetical second initiator.[32] In our simulation study for NMRP, we also proved other "microwave effect" approaches, namely, we also assumed that the MWH effect could manifest as faster thermal initiation or faster radical deactivation.[33] Although not reported, for our NMRP simulation paper we also attempted capturing the MWH effect by using a "thermal effect" approach, namely, by using kinetic rate constants corresponding to a higher (constant) temperature; however, the agreement with experimental data obtained with that modeling approach was not as good as with the other three approaches. Following our modeling approach for MI-activated RAFT polymerization,[34] Zetterlund and Perrier implemented our radical generation from monomer approach, and also tried other two approaches (modeling the polymerization at a higher temperature –a thermal effect approach-, and using simultaneously higher propagation and addition rates –a microwave effect approach-).[35] In an attempt to evaluate the validity of our proposed radical generation from monomer reaction, Sugihara et al.[27] carried out a very interesting experiment where monomer in the absence of initiator and RAFT controller was heated by MI and they did not observe formation of detectable polymer, which suggested that the formation of free radicals from monomer by MI was unlikely to occur.

From the above discussion, it is pertinent to point out that by "microwave effect" we understand the presence of an additional reaction in the polymerization scheme, or the unusually high kinetic rate constant(s) of a single or a few reactions from the overall occurring in the reaction mechanism, caused by the action of MI. "Thermal effect" refers to changes in the temperature profile of the reacting mixture, caused by MI, which affect all the reactions of the reaction mechanism.

In this contribution, we address for the first time the modeling of MI-activated ATRP of MMA and styrene using two approaches: (a) a model inspired in the "microwave effect" approach (inclusion of a reaction of radical generation from monomer), and (2) a model based on pure "thermal" effects (a model of conventional ATRP with predefined temperature profiles).

Modeling

The polymerization scheme for ATRP used in this study, as implemented in the Predici software of CiT,[36] is shown in Table 1.The reactions that make up the reaction mechanism are called "steps", as in the Predici literature.[36] Steps 1-3 and 5-15 correspond to a conventional ATRP scheme, such as the one used by Delgadillo-Velazquez and coworkers in their kinetic model for ATRP.[37] Step 4 accounts for generation of free radicals from monomer due to MI ("microwave effect").[31-34] Steps 16-21 were included to take into account induction periods which can be attributed to the presence of O_2 and impurities in the reaction system or slow formation of the catalytic centers.[6,10] Step 22 accounts for RP initiation (used for parameter estimation purposes). This polymerization scheme,which captures the effect of MI through a chemical reaction (Step 4, the so-called "microwave effect"), will bereferred to as"Model 1".

As pointed out in the introduction section of this contribution, the present dominant view in the literature on the effect of MI on the performance of RDRP is that the observed enhanced polymerization rates are due to purely "thermal" and not to

"microwave" effects.[26] So, in order to contribute to the discussion in this area, we also used a model for ATRP under MI based on purely thermal effects. To do that, we basically used the same polymerization scheme shown in Table 1, just eliminating Step 4 and providing an adequate temperature profile. Since few reports on detailed temperature profiles in ATRP under MI are usually available, we used temperature steps at specific given times. So, the time when temperature is increased and the value of the reached temperature became fitting parameters. In cases where steep temperature profiles were known to occur (when temperature was purposely increased and measured), several short temperature steps were considered in the model. This approach is referred to as "Model 2" in this contribution.In dealing with Model 2, Arrhenius expressions for all the kinetic rate constants are needed. For simplification purposes it was assumed in most of the calculations that $K=k_a/k_b$ was independent of temperature; however, calculations with $K=K(T)$ are also included in this paper in order to assess the validity of this assumption.

Except for the kinetic equations that include monomer (M) or free radicals from MI (Mic$^{\bullet}$), the kinetic equations that describe the ATRP of vinyl monomers under Model 1 are given by Equation (2)-(35) of Delgadillo-Velázquez et al.[37] The rate of monomer consumption under MI is given by Equation (1); the rate of change in the concentration of free radicals obtained from monomer due to MI is given by Equation (2), below.

$$\frac{d(V[M])}{Vdt} = -k_{dim}[M]^2 - k_{ir}[M] - k_{ia}[M][D] - k_p[M]([R^{\bullet}] + [M^{\bullet}] + [D^{\bullet}] + Y_0) -$$

9

$$k_{pz}[M][RZ^\bullet] - k_{pz}[M]S_0 - k_{fm}[M]Y_0 \tag{1}$$

$$\frac{d[VMic^\bullet]}{Vdt} = \frac{1}{2}k_{ir}[M] + k_a[MX][C] - k_b[Mic^\bullet][XC] - k_p[M][Mic^\bullet] - k_z[Z][Mic^\bullet] \tag{2}$$

Number- and weight average molecular weights, M_n and M_w, as well as the dispersity of molecular weight, Đ, were calculated in terms of the moments of the different polymer populations (living, dead and dormant polymer populations).[37]

Diffusion-controlled effectswere modeled using equilibrium free-volume theory. The effective kinetic rate constants were calculated using Equation (3), where i= a, b, dim, fd, fm, ia, p, pz, tc, td, z, namely the different reactions involving polymer molecules, which become diffusion-controlled. C_{rd} accounts for reaction-diffusion termination and is used only for i= tc and td (bimolecular termination).

$$k_i = k_i^0 \exp\left[-\beta_i\left(\frac{1}{V_f} - \frac{1}{V_{f0}}\right)\right] + C_{rd}k_p[M] \tag{3}$$

$V_f$andV_{f0}in Equation (3) are fractional free volume at time t and at initial conditions, respectively, and are calculated using Equation (4). β_i(i= a, b, dim, fd, fm, ia, p, pz, tc, td and z) in Equation (3) are free-volume parameters, T_{gk} is the glass transition temperature of component k; α_k is the expansion coefficient for species k, and $\varphi_k$is volume fraction of component k.

$$V_f = 0.025 + \sum_{k=1}^{\#\,of\,components} \alpha_k\left(T - T_{gk}\right)\varphi_k \tag{4}$$

Results and Discussion

Cases Analyzed

Eight different polymerization systems (Cases) were studied in this paper; two of them (Cases 1 and 2) are related to the ATRP of MMA and the other six (Cases 3 to 8) to the ATRP of St. Polymerization conditions for these systems are summarized in Table 2. Some of these cases were modeled more than once in order to show the effect of some kinetic parameters. Cases 1, 3 and 5 proceeded by CH. Cases 2and 4 were simulated using Model 1. Cases 6 to 8 contained sudden temperature increases and were, therefore, simulated using Model 2. In order to compare the performance of both models for the same system, Cases 2 and 6 were addressed using both Models. Tables 3 and 4 list the kinetic parameters for MMA and St used in the simulations, respectively.

ATRP of MMA by CH and MI

As stated before, Cases 1 and 2 correspond to the CHand MI (MWH) ATRP of MMA, respectively, at 69 °C,using ethyl 2-bromobutyrate (EBB) as initiator, and cupper chloride (CuCl)/N,N,N',N'',N''-pentamethyldiethylenetriamine (PMDETA) as catalyst. Case 1 was used to estimate parameters β_a, β_b, [Z], k_{pz}, k_z, and k_b(K= k_a/k_b), listed in Table 3.Model 1 was used to address Case 2.$k_{ir}$was fitted from the experimental data, to give k_{ir}= $2x10^{-8}$ s^{-1}. Regarding some of the free-volume parameters for Cases 1 and 2, the glass transition temperature of the solvent N,N-dimethylformamide(DMF) and its corresponding $\alpha_S$were assumed equal to those of

toluene.[43] The activation kinetic rate constant, k_a, for the system EBB/CuCl/PMDETA was assumed to be equal to that for the system ethyl 2-bromoisobutyrate (EtBriB)/cupper bromide (CuBr)/PMDETA[44](see Table 3), since the values of k_a for both catalysts, CuCl and CuBr, are of the same order of magnitude.[45]The β_p and β_t diffusion-controlled parameters were estimated using experimental data for bulk homopolymerization of MMA with AIBN at 70 ºC,[41]using Steps 10, 13, 14 and 22 from our Predici implementation (see Table 3). The other diffusion-controlled parameters, namely, β_j (for j= pz, z) were set equal to 0.1.

The predicted profiles of $\ln(M_0/M)$ vs. time, $M_n$vs.conversion and Đvs.conversion for Cases 1 and 2 are shown in Figure 1. Model predictionsof polymerization rate (expressed as logarithmic conversion) versus time are in very good agreement with the experimental data for both the CH and MI cases (see Figure 1a).In the case of molecular weight development (M_n vs. conversion), there is good agreement between the calculated and experimental profiles for the case of polymerization of MMA by CH (Case 1), but the calculated profile for the case under MI (Case 2) is underestimated at intermediate and high conversions (see Figure 1b).There is also some mismatch between the calculated and experimental profiles of Đ vs.conversion for both cases (see Figure 1c); the qualitative trends are preserved, but the calculate profiles lie below the experimental data in both cases. Although the model predicts rather large Đ values at very low conversions, that trend does not occur as fast and to such high values (Đ ~1.5 at very low conversions in the calculated profile) in the experimental profile. This phenomenon has also been observed in the NMRP of styrene, and it has been shown that if frequent sampling is implemented at the very early stages of the polymerization, large Đ values, with

a fast decay, are then obtained (e.g., see the experimental data of Figure 9 of Roa-Luna et al.[46]).

As discussed in our introduction section, it has been claimed in the literature that the effect of MI in polymerizations is purely thermal. So, besides using Model 1 for Case 2, several "purely thermal" simulations (Model 2) were carried out. Simulations 2b to 2d (see Figure 2) were produced with Model 2. In the case of simulation 2e, a combination of Models 1 and 2 was used (see Table 5).Simulations with Model 2were carried out by setting $k_{ir}= 0$, suddenly increasing temperature at a given time, and then proceeding isothermally again at the higher temperature. The time at which T is increased, and its new higher value, became model parameters. As mentioned before, Case 2 was addressed using both models, given the sharp increase in polymerization rate (see experimental data of Figure 2a), which suggested that the polymerization temperature likely deviated from isothermal conditions.

Although the agreement between experimental data and the predicted profile of $\ln(M_o/M)$ vs. time using Model 1 shown in Figure 1looks very good at first sight, when the time scale is expanded as in Figure 2a (Simulation 2a), it is observed that the predicted profile lies over the experimental data during the first 130 minutes, and then remains significantly below the experimental data thereafter. In the case of Simulation 2b, the polymerization proceeds very slowly during the first 83 minutes, and then increases abruptly when T is increased to 230 ^{0}C; however, the predicted profile largely overestimates the polymerization rate from 83 to 130 minutes, and then the polymerization rate is clearlyunderestimated. When T is

13

raised to 215 ^{0}C from the beginning of the polymerization (Simulation 2c), the predicted profile of ln(M_o/M) vs. time increases gradually but significantly above the experimental data during the first half (before 130 minutes) of the polymerization, and then remains below the experimental data, but closer to them than Simulations 2a and 2b. When three temperature steps are considered (Simulation 2d, Figure 2a), the agreement between calculated (with Model 2) and experimental data of ln(M_o/M) vs. time is very good, but the broken profile caused by the temperature steps clearly shows that the actual temperature profile is not stepwise. The best agreement and performance for polymerization rate is obtained with Simulation 2e, namely, with a combination of Models 1 and 2 (a lower value of k_{ir} with a temperature step not as abrupt as in simulations 2b to 2d).

In the case of predicted profiles of M_n vs. conversion, it is clearly observed in Figure 2b that calculations based on Model 1 underestimated M_n and those based on Model 2 overestimated it. The best agreement is obtained with a combination of Models 1 and 2, as in the case of Simulation 2e. The calculated profiles of Đ vs. conversion disagree significantly with the experimental data, as observed in Figure 2c. In this case, the calculations obtained with a combination of the two models outperform the performance of Model 2, but the best agreement with experimental data is obtained with Model 1.

ATRP of STY by CH and MI

Performance and Comparison of Models 1 and 2

14

Cases 3 and4 correspond toCH and MI ATRPs of styrene, respectively, at 85 °C, using 1-bromo-1-phenylethane (1-PEB)/CuCl/PMDETA. The kinetic parameters used in both cases are listed in Table 4. Case 3 was used to estimate parameters β_a, β_b, [Z] and k_b($K= k_a/k_b$)(see Table 4) which were also used in Case 4. Model 1 was used forCase 4;a value of $k_{ir}= 1\times10^{-7}s^{-1}$was obtained by data fitting.The activation coefficient, k_a, for the system (1-PEB)/CuCl/PMDETA (see Table 4) was considered to be equal to the system (1-PEB)/CuBr/PMDETA.[41]β_p and β_t were estimated fromexperimental data for bulk homopolymerization of styrene/AIBN at 80 °C.[43]k_{pz} and k_z were assumed the same as in Cases 1 and 2. The remaining free volume parameters (β_j, j=dim, fd, fm, ia, pz, z) were set equal to 0.1, a moderate value.

Figure 3 shows a comparison of calculated and experimental profiles of $\ln(M_0/M)$ vs. time (Figure 3a), M_n vs. conversion(Figure 3b) and Đ vs. conversion(Figure 3c) for Cases 3 and 4. The simulations for Cases 3 and 4(using f_{Mn}=1, with f_{Mn} defined by Equation (5), as explained below) were produced using Model 1 and agreed well with the experimental data of logarithmic conversion versus time (see Figure 3a) and Đ versus conversion (Figure 3c), but clearly underestimated the evolution of M_n (see Figure 3b). In order to improve the model performance, an initiator efficiency defined by Equation (5) was used.[16]This efficiency implied reducing the initiator concentration of Step 1 of Table 1 by multiplying it by f_{Mn}. As observed in Figure 3b, simulations obtained with Model 1 using f_{Mn}= 0.326 improved the agreement of the calculated profiles of M_n vs. conversion with the corresponding experimental data for Cases 3 and 4, respectively, but still with significant deviation

at intermediate and high conversions, and at the cost of worsening the agreement between the calculated and experimental profiles of Đ vs. conversion (see Figure 3c).

$$f_{M_n} = \frac{M_n(Theoretical)}{M_n(GPC)} \tag{5}$$

Cases 5 to 8 correspond to ATRPs of styrene using ethyl 2-bromopropionate (EBP) as initiator and CuBr/PMDETA as catalyst. Case 5 deals with a bulk polymerization of styrene by CH (no MI involved) and was used to estimate parameters k_a, K, β_a, and β_b (see Table 4). β_p and β_t were the same as in Cases 3 and 4. Also, as in Cases 3 and 4, β_j (for j=dim, fD, fm, and ia) were set equal to a moderate value of 0.1. At this point it was assumed that K was insensitive to changes in temperature, although it has been proposed in the literature that K may vary about one order of magnitude in the interval 0 to 60 ^{0}C for the ATRP of methyl acrylate (MA) using acetonitrile (MeCN)/Tris(2-pyridylmethyl)amine (TPMA) as the catalyst system.[47]Later in this paper we will analyze the validity of this assumption by carrying out some calculations with K as a function of T. The activation coefficient, k_a, for the system EBP/CuBr/PMDETA was assumed equal to that for methyl 2-bromopropionate (MBP)/CuBr/PMDETA (see Table 4) since steric effects do not affect significantly this parameter.[41]Cases 6-8 were addressed using Model 2 since abrupt changes in polymerization rate (expressed as logarithmic conversion vs. time) were observed in the experimental profiles.[5]Results are shown in Figure 4. Case 6 was also analyzed using Model 1, in order to provide a sound and fair comparison between the two models (see Figure 5).

As in Case 2 (Simulations 2b-2e), Cases 6-8 were modeled using temperature steps at some given times (Model 2). The size of the step (temperature increase) and the time at which the step occurred were used as fitting parameters. As stated before, Simulation 6a was addressed using Model 1,for comparison purposes, and Simulation 6c was carried out using a combination of both models in order to improve the agreement between model predictions and the available experimental data. The temperature steps, their time of occurrence, and the values of k_{ir} for Model 1 (for Simulations 6a and 6c) are summarized in Table 6. As observed in Figure 4, the agreement between calculated and experimental profiles of $\ln(M_0/M)$ vs. time (Figure 4a), M_n vs. conversion (Figure 4b) and Đ vs. conversion (Figure 4c) for CH and MI ATRPs of St is very good for Cases 5, 7 and 8, and fairly good for Case 6, since the sudden increase in polymerization rate in Case 6 is predicted to occur significantly earlier with Model 2. The temperatures reached in Cases 6-8 are consistent with the temperatures measured using infrared (IR) sensors by some experimenters.[23, 30]

A comparison of the performance of Models 1 and 2 for Case 6 is shown in Figure 5. It is clearly observed that Model 1 overestimates polymerization rate (Figure 5a), slightly underestimates the evolution of M_n (Figure 5b), and slightly overestimates the evolution of Đ. Model 2, on the other hand, produced profiles that agree fairly well with the experimental data for polymerization rate (Figure 5a), and very well for the evolution of M_n (Figure 5b) and Đ (Figure 5c). The combination of both models (a low k_{ir} and rather lower temperature step) produced intermediate profiles between the two of them that improved the performance of Model 1, but were not

17

as good as Model 2.

On the Validity of Radical Generation from Monomer by MI

As explained in our introduction section, Sugihara et al.[27] carried out an experiment where monomer was heated by MI (fixed power mode of 300 W at approximately 90 ^{0}C) and they did not observe formation of detectable polymer, which suggested that the formation of free radicals from monomer by MI was unlikely to occur. We carried out a few simulations inspired in this experiment (see Figures 6 and 7, as well as Table 7). First, we calculated the concentrations of several free radical populations, namely, total living polymer ([P$^\bullet$]), initiator free radicals ([R$^\bullet$]), and free radicals from monomer by MI ([Mic$^\bullet$]), for three situations: (a) ATRP of St by MI using Model 1 (Simulation 6a, Figure 6a), (b) ATRP of St by MI using a combinations of Models 1 and 2 (Simulation 6c, Figure 6b), and (c) ATRP of MMA using Model 1 (Simulation 2a, Figure 6c). It is clearly observed that the concentration of free radicals produced from monomer by MI under Model 1 for the ATRP of St is two orders of magnitude lower than the total concentration of living polymer (10^{-9} and 10^{-10}mol L^{-1} when a combination of Models 1 and 2 is used, Figures 6a and 6b, respectively), and three orders of magnitude for the case of ATRP of MMA (Figure 6c). This level of concentration is very difficult to measure experimentally (e.g., by using electron paramagnetic resonance (EPR) spectroscopy),[48,49] where the standard is measuring concentrations in the order of 10^{-7} (total living polymer in conventional radical polymerization),[48] 10^{-4} (stable free radicals in NMRP),[49] or 10^{-3}mol L^{-1} (copper II species in ATRP).[48] Second, we simulated the bulk polymerization of St under MI, without initiator or controller, at

18

90 ^{0}C, at different values of k_{ir}, considering that microwave power (300 W) in our Model 1 is input through k_{ir}, to calculate how much polymer would be expected at the conditions of the experiments of Sugihara et al.[27]The results are summarized in Figure 7 and Table 7.

Since we did not obtain a correlation between MI power and the value of k_{ir} for the ATRP of St studied before in this paper, we simulated the conventional polymerization of Sugihara et al.[27]by using values of k_{ir} in the interval 10^{-12} to 10^{-7} s^{-1}, representative of the values used for Cases 6a & 6c, as shown in Table 7. It is observed that the concentrations of free radicals from monomer by MI are very low as to be measured by EPR. In the cases with k_{ir}= 10^{-9} and 10^{-12} s^{-1}, the conversions reached at 125 minutes (which is roughly the time used in the experiments of Sugihara et al.[27]) are low enough as to produce polymer undetected by conventional gravimetric procedures. The cases with higher values of k_{ir} predict polymer formation high enough as to be easily detectable by gravimetric procedures. So, if Model 1 is correct, the value of k_{ir} corresponding to the polymerization of St by MWH should be lower than 10^{-9} s^{-1}. Figure 7 shows the predicted profiles of $\ln(M_0/M)$ vs. time, M_n vs. conversion, and Đ vs. conversion for the case with k_{ir}= 10^{-9} s^{-1}; the polymerization proceeds slowly, probably undetectable by conventional gravimetric procedures in the first couple of hours. So, the fact that Sugihara et al.[27] did not observe formation of detectable polymer at 120 minutes, cannot be considered as a definite argument against free radical formation from monomer by MI; namely, more direct evidence is needed to either support or reject Model 1. One possibility would be to use more statistically sound techniques, such as model discrimination techniques.[50]

Calculations with K=K(T)

As mentioned before, it has been reported in the literature that K may depend on temperature for the ATRP of MA.[47] In section "Performance and Comparison of Models 1 and 2", the simulations for Cases 5-8 were carried out by assuming that K is insensitive to changes in temperature. In this section we remove that assumption by fitting k_b (remind that $K=k_a/k_b$ and that k_a has been assumed temperature-dependent, as shown in Table 3 and 4 for MMA and Sty, respectively) to the experimental data of (logarithmic) conversion versus time for Cases 5-8 (T= 80, 95, 98, and 110 ^{0}C), using the first four data points in each case, namely, using the experimental data prior to the apparent temperature rise observed in those experiments. The fitted values of k_b are included in Table 4, the new values of T_f and time of change are reported in Table 8, and the simulations carried out with the new parameters are shown in Figure 8. The new final temperatures (T_f) are roughly10°C lower than those for constant K. It is observed in Figure 8 that the agreement between calculated profiles and experimental data for polymerization rate (Figure 8a) and Đ versus conversion (Figure 8c) is quite good and better than the case with constant K (compare the results of Figures 8 and 4). However, the predicted profiles of M_n versus conversion for Cases 6 and 8 deviate (decrease) significantly from the experimental data after about 50% monomer conversion (see Figure 8b).

Conclusion

Two modeling approaches were successfully applied to the ATRP of MMA and St under MI using Predici. Model 1 was a "microwave effect" model and considered a reaction of production of free radicals from monomer by MI. Model 2 was "purely thermal" and consisted of single or multiple temperature steps at specific times. Both models were equally good in terms of agreement between experimental data and predicted profiles of logarithmic conversion versus time, and evolution with conversion of M_n and Đ.

The arguments provided by some leading scientists clearly indicate that many polymerizations carried out by MWH are non-isothermal, and thermal profiles should definitely be taken into account in modeling studies. However, although plausible, there is still no definite evidence that the "microwave effect" is inexistent. As a matter of fact, the combination of "microwave" and "purely thermal" effects is possible.

More detailed experimental studies are needed to prove that free radicals from monomer by MI are not produced. Model discrimination techniques could also provide some light into this discussion.

Keywords: Atom transfer radical polymerization ATRP;controlled radical polymerization; kinetics (polym.); microwave effect; microwave irradiation; reversible-deactivation radical polymerization.

Nomenclature

[ ]	Denotes concentration in $molL^{-1}$
C	Catalyst
D	Dimer
$D^\bullet$	Dimeric free radical
D(s)	Dead polymer molecule of size s
DimX	Halide of dimer
f_{Mn}	Initiator efficiency for reversible initiation
f	Initiator efficiency for radical initiation
ka^0	Activation kinetic rate constant
kb^0	Deactivation kinetic rate constant
K	Equilibrium constant
$kdim^0$	kinetic rate constant for the dimerization reaction
kfd^0	Transfer to dimer kinetic rate constant
kfm^0	Transfer to monomer kinetic rate constant
kia^0	Kinetic rate constant for thermal initiation
kir^0	Kinetic rate constant for microwave activation
kp^0	Propagation kinetic rate constant
kpz^0	Kinetic rate constant for propagation of inhibited radical
ktc^0	Termination by combination kinetic rate constant
ktd^0	Termination by disproportionation kinetic rate constant
kz^0	Kinetic rate constant for inhibition reaction
M	Monomer
$M^\bullet$	Monomeric free radical
MX	Halide of monomer

P(s)	Polymer free radical of size s
PX(s)	Dormant polymer molecule of size s
PZ(s)	Inhibited high molecular weight radical of size s
R$^\bullet$	Primary free radical from initiator
RX	Initiator
RZ$^\bullet$	Inhibited low molecular weight radical
T	Temperature
T$_f$	Final temperature
XC	Deactivator
Z	Inhibitor

References

[1]   A. D. Jenkins, R. G. Jones, G. Moad, *Pure Appl. Chem.* **2010**, *82*, 483.

[2]   K. Matyjaszewski, *Macromolecules* **2012**, *45*, 4015.

[3]   J. Nicolas,Y. Guillaneuf,C. Lefay, D. Bertin, D. Gigmes, B. Charleux, *Prog. Polym. Sci.* **2012**, http://dx.doi.org/10.1016/j.progpolymsci.2012.06.002

[4]   G. Moad, E. Rizzardo, S. H. Thang, *Aust. J. Chem.* **2012**, *65*, 985.

[5]   P. Marcasuzaa, S. Reynaud, B. Grassl, H. Preud'homme, J.Desbrières, M. Trchovà, O. F. X. Donard, *Polymer* **2011**, *52*, 33.

[6]   C. Hou, Z. Guo, J. Liu, L. Ying, D. Geng, *J. Appl. Polym. Sci.* **2007**, *104*, 1382.

[7]   S. Delfosse, Y. Borguet, L. Delaude, A. Demonceau, *Macromol. Rapid Commun.* **2007**, *28*, 492.

[8]   N. Li, J. Lu, Q. Xu, X. Xia, L.Wang, *Eur. Polym. J.* **2007**, *43*, 4486.

[9]   C. Hou, R. Qu, C. Ji, C. Wang, C. Sun, *J. Appl. Polym. Sci.* **2006**, *101*, 1598.

[10]   Z. Cheng, X. Zhu, N. Zhou, J. Zhu, Z. Zhang, *Radiat. Phys. Chem.* **2005**, *72*, 695.

[11]   X. Li, X. Zhu, Z. Cheng, W. Xu, G. Chen, *J. Appl. Polym. Sci.* **2004**, *92*, 2189.

[12]   H. Zhang, U. S. Schubert, *Macromol. Rapid Commun.* **2004**, *25*, 1225.

[13]   Z. Cheng, X. Zhu, M. Chen, J. Chen, L. Zhang, *Polymer* **2003**, *44*, 2243.

[14]   G. Wang, X. Z. Hu, Z. Cheng, N. Z. Hou, J. Lu, *Polymer* **2003**, *35*,399.

[15]   W. Xu, X. Zhu, Z. Cheng, G. Chen, J. Lu, *Eur. Polym. J.* **2003**, *39*, 1349.

[16]   X. Zhu, N. Zhou, X. He, Z. Cheng, J. Lu, *J. Appl. Polym.Sci.* **2003**, *88*, 1787.

[17]   D. Roy, B. S. Sumerlin, *Polymer* **2011**, *52*, 3038.

[18]   C. T. Nguyen, Q. D. Nghiem, D. Kim, J. S.Chang, Y. K.Hwang, *Polymer* **2009**, *50*, 5037.

[19]   D. Roy, A. Ullah, B. S.Sumerlin, *Macromolecules* **2009**, *42*, 7701.

[20]   Y. Assem, A. Greiner, S. Agarwal, *Macromol. Rapid Commun.* **2007**, *28*, 1923.

[21]   S. L. Brown, C. M. Rayner, S. Perrier, *Macromol. Rapid Commun.* **2007**, *28*, 478.

[22]   J.Zhu, X.Zhu, Z.Zhang, Z.Cheng, *J. Polym. Sci., Polym. Chem.* **2006**, *44*, 6810.

[23]   J. Rigolini, B. Grassl, S. Reynaud, L. Billon, *J. Polym. Sci., Polym.Chem.* **2010**, *48*, 5775.

[24]   J. Rigolini, B.Grassl, L.Billon, S. Reynaud, O. F. X. Donard, J. *Polym. Sci., Polym. Chem.* **2009**, *47*, 6919.

[25]   J. Li, X. Zhu, J. Zhu, Z. Cheng, *Radiat. Phys. Chem.* **2007**, *76*, 23.

[26]   Y. Kwak, R. T. Mathers, K. Matyjaszewski, *Macromol.RapidCommun.* **2012**, *33*, 80.

[27]   Y. Sugihara, M. Semsarilar, S.Perrier, P. B. Zetterlund, Polym. Chem. **2012**, 3, 2801.

[28]   Z. Cheng, X. Zhu, G. Chen, W. Xu, J. Lu, *J. Polym. Sci., Part A: Polym. Chem.* **2002**,*40*,3823.

[29]   G. Chen, X. Zhu, Z. Cheng, J. Lu, Chen, J. *Polym. Int.* **2004**, *53*, 357.

[30]   M. A. Herrero, J. M. Kremsner, C. O. Kappe, *J. Org. Chem.* **2008**, *73*, 36.

[31]   M. A. Aldana-García, J. Palacios, E. Vivaldo-Lima, *J. Macromol. Sci., Part A: Pure Appl. Chem.* **2005**, *42*, 1207.

[32]   G. Jaramillo-Soto, M. Ramírez-Cupido, J. A. Tenorio-López, E. Vivaldo-Lima, A. Penlidis, *Chem. Eng. Technol.* **2010**, *33*, 1888.

[33]   J. J. Hernández-Meza, G. Jaramillo-Soto, P. R. García-Morán, J. Palacios-Alquisira, E. Vivaldo-Lima, *Macromol. React. Eng.***2009**, *3*, 101.

[34]   J. C. Hernández-Ortiz, G. Jaramillo-Soto, J. Palacios-Alquisira, E. Vivaldo-Lima, *Macromol. React. Eng.* **2010**, *4*, 210.

[35]   P. E. Zetterlund, S. Perrier, *Macromolecules* **2011**, *44*, 1340.

[36]   M. Wulkow, *Macromol. React. Eng.* **2008**, *2*, 461-494.

[37]   O. Delgadillo-Velázquez, E.Vivaldo-Lima, I. A. Quintero-Ortega, S. Zhu, *AIChE J.* **2002**, *48*, 2597.

[38]   S. Ahn, S. Chang, H. Rhee, *J. Appl. Polym.Sci.* **1998**, *69*, 59.

[39]   S. Beuermann, M. Buback, *Prog. Polym. Sci.* **2002**, *27*, 191.

[40]   M. Zhang, W. H. Ray, *Ind. Eng. Chem. Res.* **2001**, *40*, 4336.

[41]   F. Seeliger, K. Matyjaszewski, *Macromolecules* **2009**, *42*, 6050.

[42]   E. Vivaldo-Lima, R.García-Pérez, O. J. Celedón-Briones, *Rev. Soc. Quim.Mex.* **2003**, *47*, 22.

[43]   E. Vivaldo-Lima, A. E. Hamielec, P. E. Wood, *Polym. React. Eng.* **1994**, *2(1&2)*, 17.

[44]   J. Belicanta-Ximenes, P. V. R. Mesa, L. M. F. Lona, E. Vivaldo-Lima, N. T. McManus, A. Penlidis, *Macromol. TheorySimul.* **2007**, *16*, 194-208.

[45]   A. Goto, T. Fukuda, *Macromol. Rapid Commun.* **1999**, *20*, 633.

[46]   M. Roa-Luna, A.Nabifar, M. P. Díaz-Barber, N. T. McManus, E.Vivaldo-Lima, L. M. F. Lona, A. Penlidis, *J. Macromol. Sci., Pure Appl. Chem.* **2007**, *44*, 337.

[47]   Y. Wang, Y. Kwak, J. Buback, M. Buback, K. Matyjaszewski, *ACS Macro Lett*. **2012**, 1, 1367.

[48]   A. Kajiwara, K. Matyjaszewski, M. Kamachi,Macromolecules **1998**, *31*, 5695.

[49]   D. Benoit, S. Grimaldi, S. Robin, J.-P. Finet, P.Tordo, Y. Gnanou, *J. Am. Chem. Soc.* **2000**, *122*, 5929.

[50]   S. Masoumi, T. A. Duever, P.M. Reilly, *Can. J. Chem. Eng.* **2013**, 91(5), 862.

Tables

Table 1. Model implementation in Predici

Reaction	Step	Name of step	Kinetic rate constant	Step #
Initiation	RX+C ↔R$^\bullet$+XC	Reversible reaction	k_a, k_b	1
Mayo dimerization	M+M →D	Elemental reaction	k_{dim}	2
Thermal initiation	D+M →M$^\bullet$+D$^\bullet$	Elemental reaction	k_{ia}	3
Microwave-promoted initiation	M→ 2Mic$^\bullet$	Elemental reaction	k_{ir}	4
Monomeric radical deactivation	MX+C ↔M$^\bullet$+XC MX+C ↔Mic$^\bullet$+XC	Reversible reaction	k_a, k_b	5
Dimeric radical deactivation	DX+C ↔D$^\bullet$+XC	Reversible reaction	k_a, k_b	6
First propagation	R$^\bullet$ + M→ P(1)	(Anionic) initiation step	k_p	7
First propagation	M$^\bullet$ + M→ P(1) Mic$^\bullet$ + M→ P(1)	(Anionic) initiation step	k_p	8
First propagation	D$^\bullet$ + M→ P(1)	(Anionic) initiation step	k_p	9
Propagation	P(s)+ M →P(s+1)	Propagation	k_p	10
Dormant-living exchange (Deactivation)	P(s) + XC →PX(s)+C	Change	k_b	11
Dormant-living exchange (Activation)	PX(s) + C →P(s)+C	Change	k_a	12
Termination	P(s)+ P(r) →D(r+s) P(s) +P(r) → D(s)+D(r)	Combination/ Disproportionation	k_{tc} k_{td}	13
Chain transfer to monomer	P(s)+M →D(s)+ M$^\bullet$	Change	k_{fm}	14

Chain transfer to dimer	$P(s)+D \rightarrow D(s)+ D^\bullet$	Change	k_{fd}	15
Inhibition of primary free radical	$R^\bullet+Z \rightarrow RZ^\bullet$	Elemental	k_z	16
Inhibition of dimeric radical	$D^\bullet+Z \rightarrow RZ^\bullet$	Elemental	k_z	17
Inhibition of monomeric radical	$M^\bullet+Z \rightarrow RZ^\bullet$ $Mic^\bullet+Z \rightarrow RZ^\bullet$	Elemental	k_z	18
Inhibition of living polymer	$P(s)+Z \rightarrow PZ(s)$	Change	k_z	19
Propagation of inhibited radical	$RZ^*+M \rightarrow P(1)$	(Anionic) initiation step	k_{pz}	20
Propagation of inhibited polymer	$PZ(s)+M \rightarrow P(s+1)$	Propagation (copolymer)	k_{pz}	21
Chemical Initiaton	$I \rightarrow 2R^\bullet$ $R^\bullet + M \rightarrow P(1)$	Radical initiation	k_d, f	22

Table 2. ATRP systems studied in this paper

Case	Heating	Mono-mer	Initiator/Catalyst	Solvent	[M]/[RX]/[C]	S/M (v/v)	T (°C)	Power (W)	Refe-rence
1	CH	MMA	EBB/CuCl/PMDETA	DMF	2400/1/2	1/5	69	0	[13]
2	MWH	MMA	EBB/CuCl/PMDETA	DMF	2400/1/2	1/5	69	360	[13]
3	CH	Sty	1-PEB/CuCl/PMDETA	DMF	100/1/1	1/5	85	0	[10]
4	MWH	Sty	1-PEB/CuCl/PMDETA	DMF	100/1/1	1/5	85	12	[10]
5	CH	Sty	EBP/CuBr/PMDETA	Bulk	400/1/1	0	95	0	[5]

6	MWH	Sty	EBP/CuBr/PMDETA	Bulk	400/1/1	0	98	80	[5]
7	MWH	Sty	EBP/CuBr/PMDETA	Bulk	400/1/1	0	110	100	[5]
8	MWH	Sty	EBP/CuBr/PMDETA	Bulk	400/1/1	0	80	80	[5]

Table 3. Kinetic and physical parameters used in the simulations for MMA(T in K)

Parameter	Units	Value	Reference
k_{fm}^0	L mol^{-1}s^{-1}	$9.32\times 10^4\exp(-6986/T)$	[38]
k_p^0	L mol^{-1}s^{-1}	$2.39\times10^6\exp(-2669/T)$	[39]
k_t^0	L mol^{-1}s^{-1}	$5.2\times 10^8\exp(-697/T)$	[38]
k_{td}^0/k_{tc}^0	Dimensionless	$2.483 \times 103\ \exp(-2036/T)$	[40]
k_a^0, Kfor EBB/CuCl/PMDETA	L mol^{-1}s^{-1}, Dimensionless	$1.63\times10^5\exp(-3308/T)$, 2.06×10^{-7}	[41], This work
k_z, k_{pz}	L mol^{-1}s^{-1},	1×10^6, 5.5×10^{-6}	This work
[Z]	mol L^{-1}	1×10^{-3}	This work
C_{rd}	L mol^{-1}	1.12	[42]
T_{gm}, T_{gp}, T_{gs}	°C	-106, 114, -160	[38], [38], [43]
α_m, α_p, α_s	K^{-1}	1×10^{-3}, 4.8×10^{-4}, 7×10^{-3}	[38], [38],[43]
β_p, β_t	Dimensionless	0.33, 1.45	This work
β_a, β_b for EBB/CuCl/PMDETA	Dimensionless	2.5, 4	This work

Table 4. Kinetic and physical parameters used in the simulations for St(T in K)

Parameter	Units	Value	Reference
k_{dim}^0	L mol^{-1}s^{-1}	$188.97\exp(-8133/T)$	[44]
k_{fd}^0	L mol^{-1}s^{-1}	50	[44]
k_{fm}^0	L mol^{-1}s^{-1}	$9.376 \times10^{6}\exp(-6720)$	[44]
k_{ia}^0	L mol^{-1}s^{-1}	$6.359 \times10^{12}\exp(-$	[44]

		18391/T)	
k_p^0	L mol^{-1}s^{-1}	4.27×10^{7}exp(-3909)	[39]
k_{tc}^0	L mol^{-1}s^{-1}	1.06 ×10^{9}exp(-753)	[39]
k_a^0, Kfor 1-PEB/CuCl/PMDETA	L mol^{-1}s^{-1}, Dimensionless	2.97×10^{5}exp(-4378/T), 3.24× 10^{-9}	[41], This work
k_a^0,$k_b^0$for EBP/CuBr/PMDETA	L mol^{-1}s^{-1}, L mol^{-1}s^{-1}	1.2×10^{5}exp(-3993/T), 5.83×10^{15}exp(-7001/T)	[41], This work
k_z,k_{pz}(Case 3&4)	L mol^{-1}s^{-1}	1×10^6, 5.5×10^{-6}	This work
[Z](Case 3&4)	mol L^{-1}	1.4×10^{-2}	This work
C_{rd}	L mol^{-1}	135	[43]
T_{gm}, T_{gp},T_{gs}	°C	-88, 100,-160	[43]
α_m, α_p, α_s	K^{-1}	1× 10^{-3}, 4.8×10^{-4}, 7×10^{-3}	[43]
β_p,β_t	Dimensionless	0.1, 0.34	This work
β_a,β_b for1-PEB/CuCl/PMDETA	Dimensionless	2.5, 6	This work
β_a,β_b forEBP/CuBr/PMDETA	Dimensionless	0.2, 0.5	This work

Table 5. Temperature conditions for Case 2

Simulation	Case	Initialtemperature (°C)	Final temperature,T_f (°C)	Time of change(min)	k_{ir} (s^{-1})
2a	2	69	69	0	2×10^{-8}
2b	2	69	230	83.3	0

|					
2c	2	69	215	0	0
2d	2	69	110, 230, 340	50, 116.7, 150	0
2e	2	69	125	137.5	1.35×10^{-8}

Table 6. Temperature step changes and times of occurrence for Cases 5 (CH) and 6-8 (MI)

Simulation	Case	Initial temperature (°C)	Final temperature, T_f (°C)	Time of change (s)	k_{ir} (s^{-1})
5	5	95	95	0	0
6a	6	98	98	0	1×10^{-6}
6b	6	98	180	3000	0
6c	6	98	170	5000	1×10^{-12}
7	7	110	190	2800	0
8	8	80	170	8000	0

Table 7. Effect of parameter k_{ir} on Conversion, M_n and [Mic$^\bullet$] at 125 minutes, in the MI bulk polymerization of St at 90 ^{0}C, using Model 1

k_{ir} (s^{-1})	Conversion	M_n (g mol^{-1})	[Mic$^\bullet$] (mol L^{-1})
1×10^{-12}	2.35×10^{-3}	1.05×10^{6}	3.54×10^{-14}
1×10^{-9}	7.09×10^{-2}	5.27×10^{5}	3.24×10^{-12}
1×10^{-8}	0.2	2.43×10^{5}	2.52×10^{-11}
1×10^{-7}	0.48	8.43×10^{4}	2.29×10^{-10}

Table 8. Temperature step changes and times of occurrence for Cases 5 (CH) and 6-8 (MI)

| Case	Initial temperature (°C)	Final temperature, T_f (°C)	Time of change (s)	k_{ir} (s^{-1})
5	95	95	0	0
6	98	170	3000	0
7	110	180	2800	0
8	80	165	8000	0

Figures
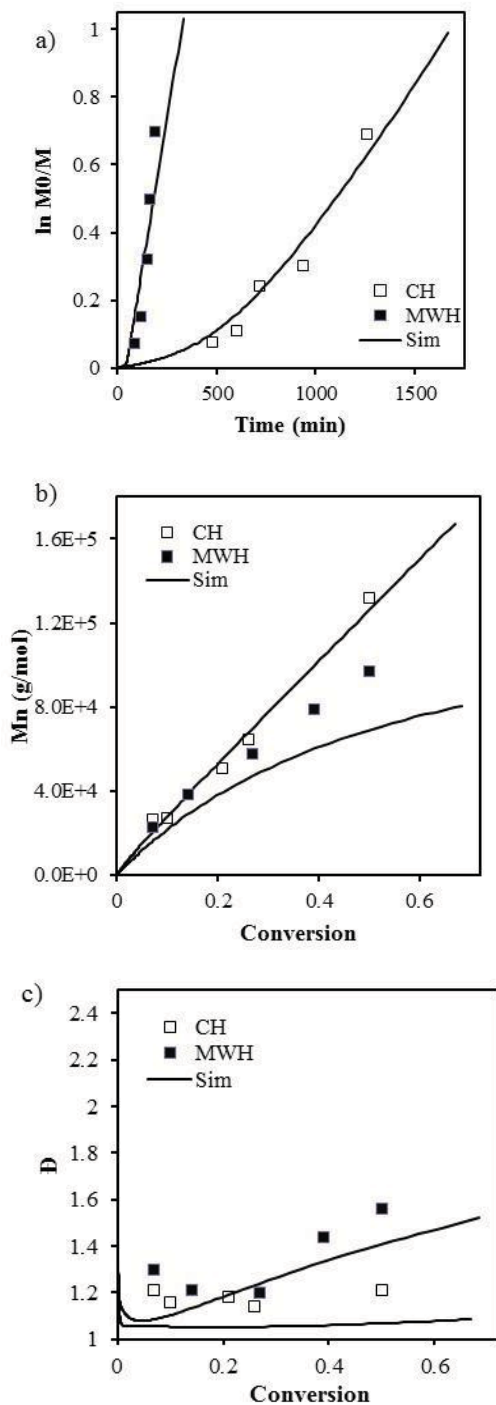
Figure 1. CH (Case 1, □) and MI (Case 2, ■) ATRP of MMA in DMF at 69 ^{0}C. Comparison of predicted profiles of (a) ln(M$_0$/M) vs. time, (b) M$_n$vs. conversion, and (c) Đvs.conversion, using Model 1,against experimental data.Empty symbols representCH and full symbols MI polymerizations.
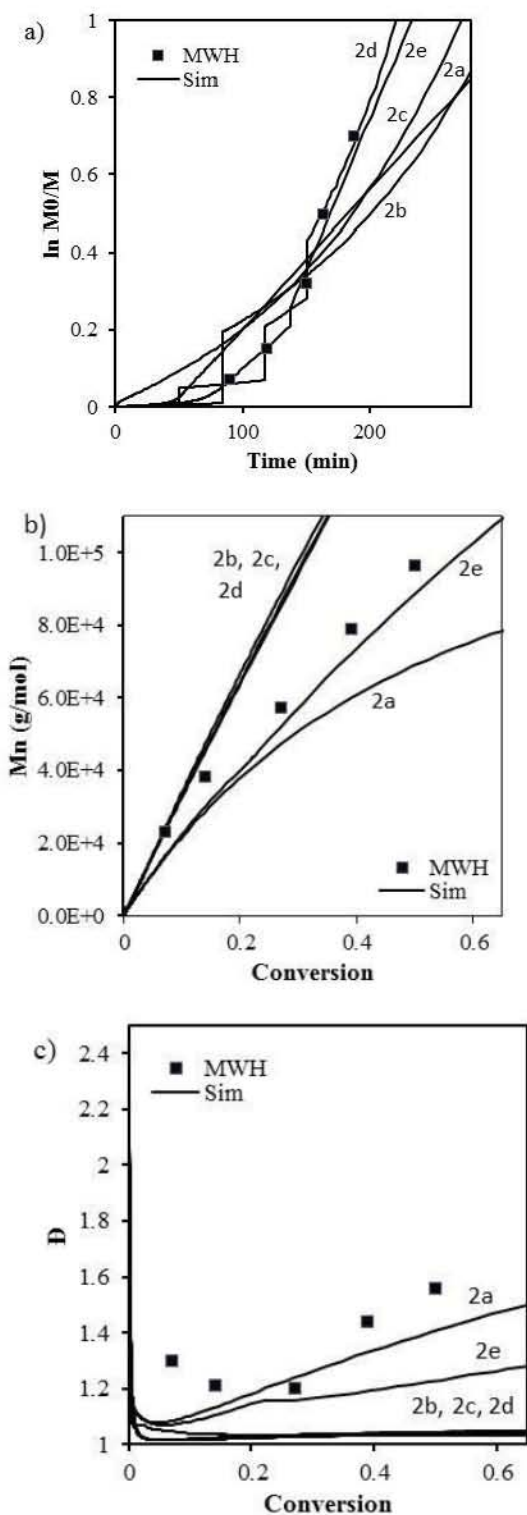
Figure 2. Simulations of MI ATRP of MMA in DMF at 69 ^{0}C (Case 2, ■) using Models 1 (Profile 2a), 2 (Profiles 2b to 2d), and a combination of both (Profile 2e).See Table 5 for other polymerization conditions.
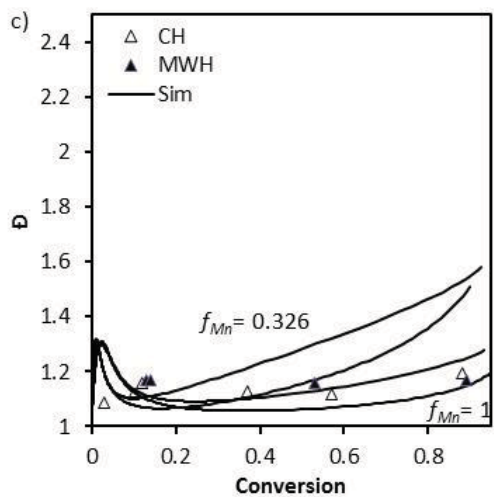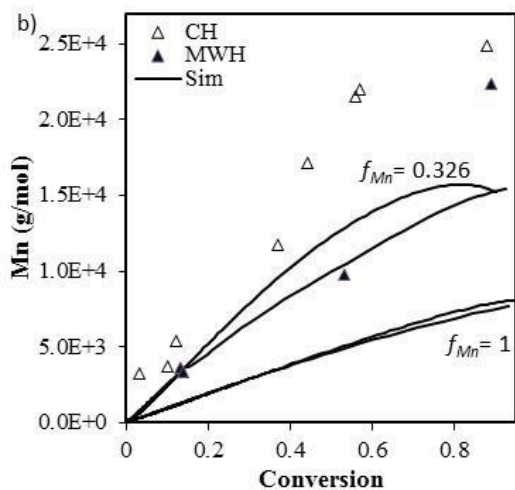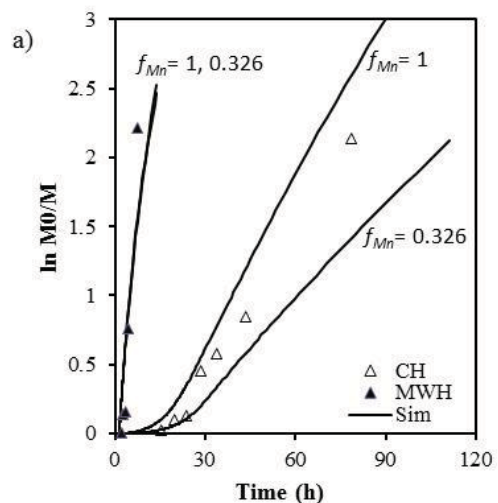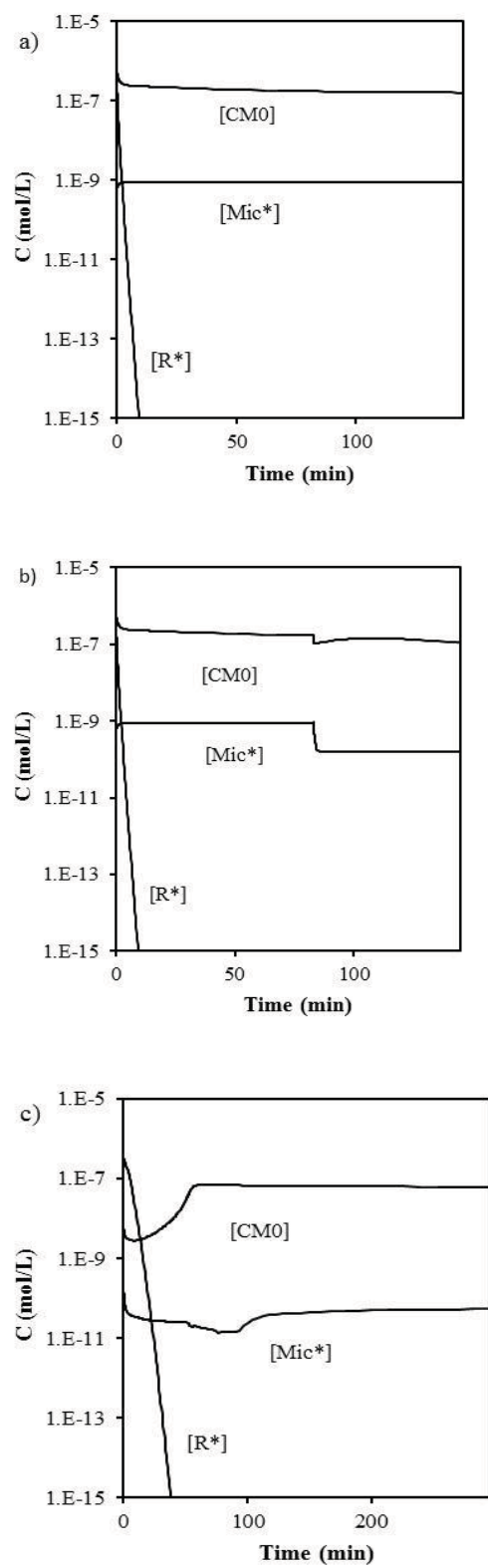
Figure 3. Comparison of experimental and calculated profiles, using Model 1, of (a) $\ln(M_0/M)$ vs. time, (b) M_n vs. conversion and (c) Đ vs. conversion, for CH (Case 3, △) and MI (Case 4, ▲) ATRPs of St in DMF at 85 ^{0}C.
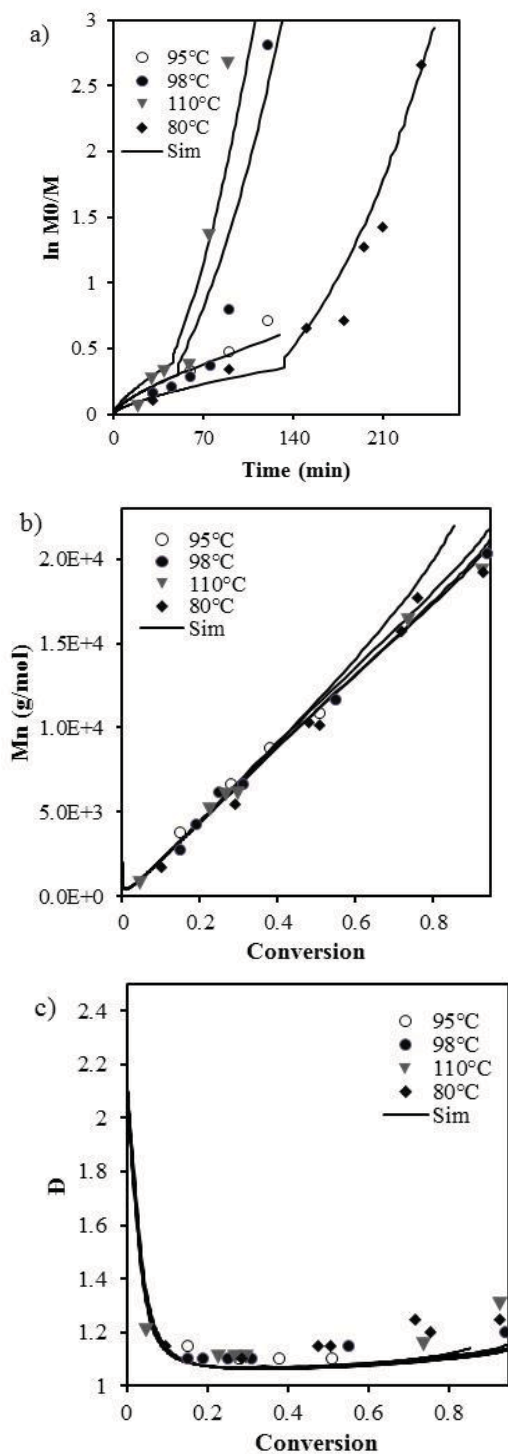
Figure 4. Comparison of experimental and calculated profiles, using Model 2, of (a) ln(M$_0$/M) vs. time, (b) M$_n$ vs. conversion and (c) Đ vs. conversion, for CH (Case 5,○) and MI (Case 6, ●; Case 7, ▼; and Case 8, ♦) ATRPs of St at different temperatures.
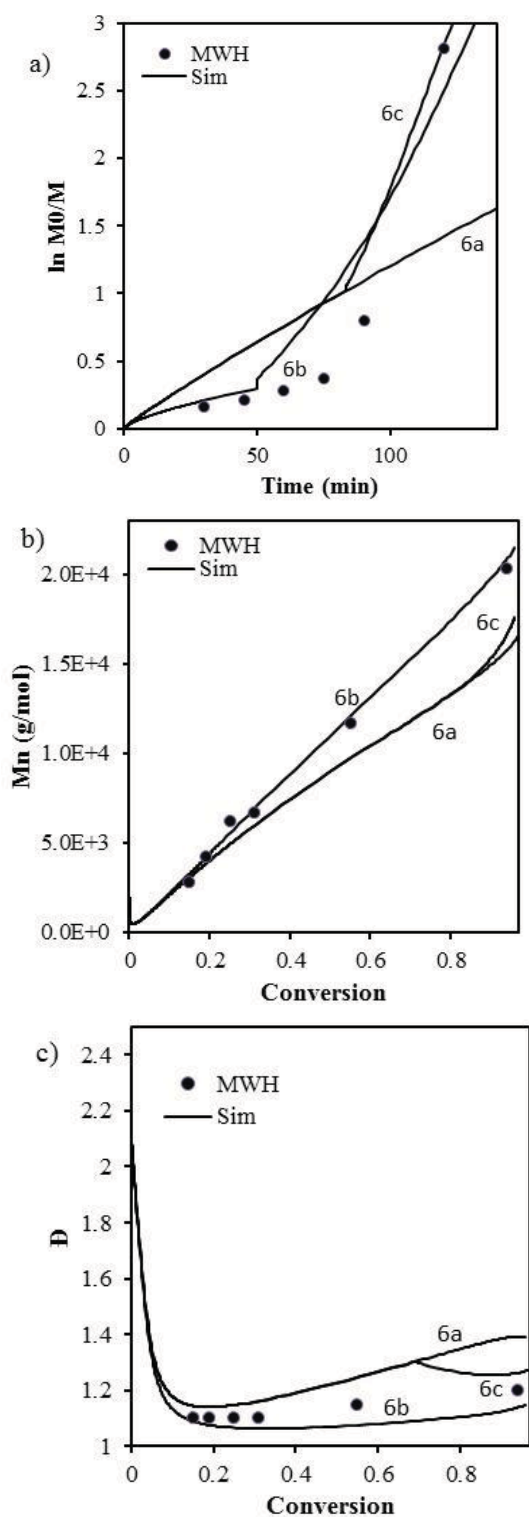
Figure 5. Comparison of the performance of Models 1 (Simulation 6a), 2 (Simulation 6b) and a combination of both (Simulation 6c) for the ATRP of St by MI at 80 W and 98 ^{0}C (Case 6,●): (a) ln(M_0/M) vs. time, (b) M_n vs. conversion and (c) Đ vs. conversion. See Table 6 for other polymerization conditions).

Figure 6. Calculated concentrations of free radicals for: (a) Case 6 (St) using Model 1 (Simulation 6a), (b) Case 6 (St) using Models 1 and 2 (Simulation 6c), and

(c) Case 2 (MMA) using Model 1 (Simulation 2a).
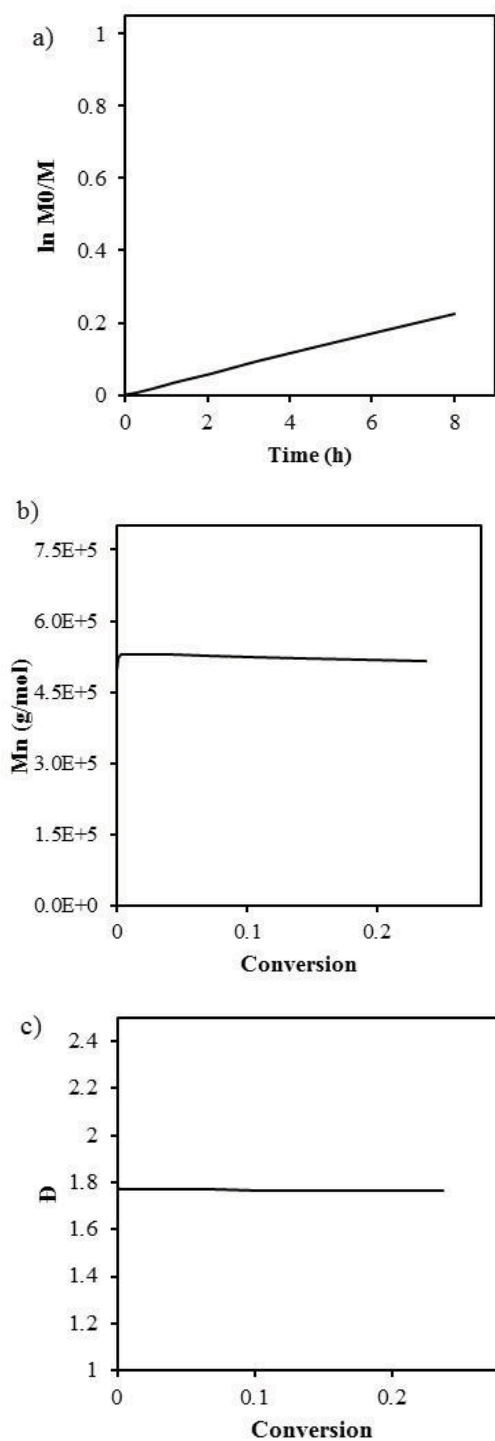
Figure 7. Calculated profiles of (a) ln(M0/M) vs. time, (b) M_n vs. conversion and (c) Đ vs. conversion, for the bulk polymerization of St under MI, without initiator or controller, using Model 1 with $k_{ir}= 10^{-9}$ s^{-1}.
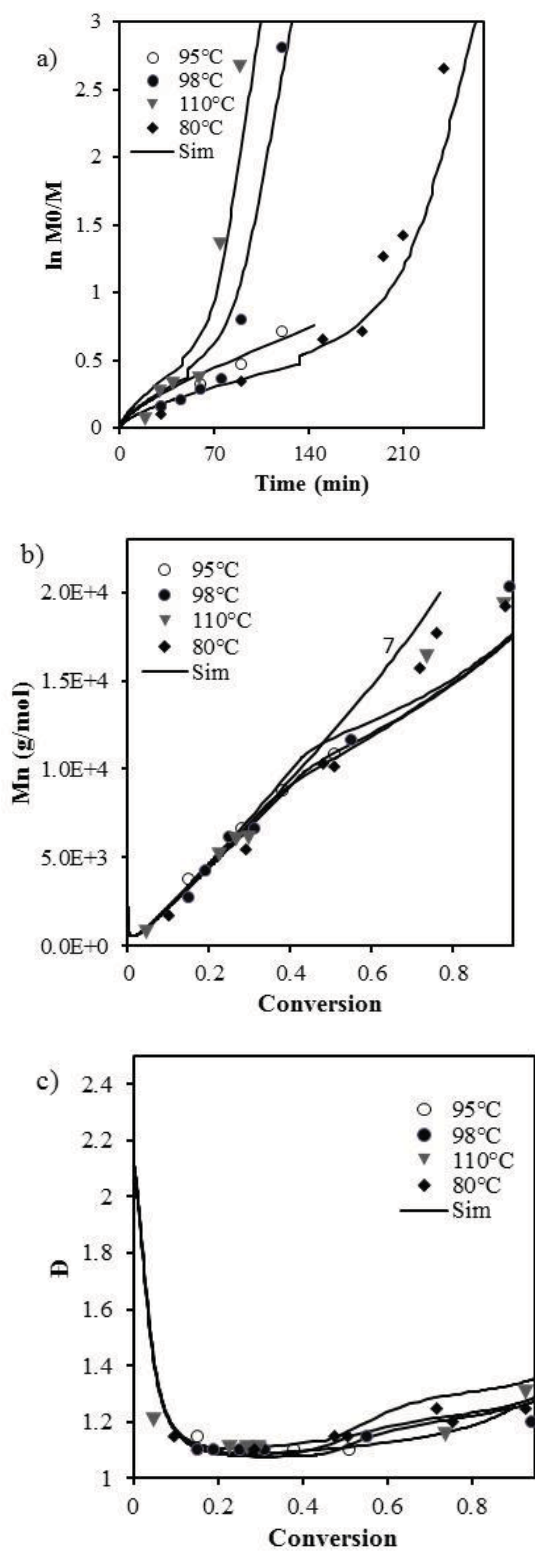
Figure 8. Comparison of experimental and calculated profiles, using Model, of (a) ln(M_0/M) vs. time, (b) M_n vs. conversion and (c) Đ vs. conversion, for CH (Case 5,○) and MI (Case 6, ●; Case 7, ▼; and Case 8, ♦) ATRPs of St with K= K(T).